Available online at www.sciencedirect.com
ScienceDirect
Infrared Physics & Technology 50 (2007) 227–233
INFRARED PHYSICS & TECHNOLOGY
www.elsevier.com/locate/infrared

Research topics at Thales Research and Technology: Small pixels and third generation applications

Alexandru Nedelcu *, Eric Costard, Philippe Bois, Xavier Marcadet

Alcatel-Thales III-V Lab, Groupement d'Intérêt Economique, Route Départementale 128, 91767, Palaiseau Cedex, France

Available online 14 November 2006

Abstract

Recent results obtained on building blocks for future third generation infrared focal plane arrays (FPAs) are presented. Our approach concerning the FPA performance assessment and small pixels modelling is exposed. We also demonstrate the ability of the quantum well infrared photodetector technology to answer the needs for compact (20 μm pitch) polarimetric FPAs. Finally, we present our first results on mid-wave infrared detectors at wavelengths below 4.2 μm.

1. Introduction

Quantum-well infrared photodetectors (QWIPs) have been widely investigated for detection in the mid (3–5 μm) and long-wavelength (8–14 μm) infrared (IR) atmospheric spectral windows. Their specific advantages (III–V materials, narrow spectral response, easy wavelength adjustment, high thermal stability, high uniformity and yield, no low-frequency noise) established them as a serious candidate for third generation thermal imagers [1–3].

At Thales Research and Technology (TRT) research on QWIPs has always been driven by the needs and constraints set by the operational systems. Reliable IR cameras for Thales applications need high temperature operation ($T_{FPA} > 73$ K), low integration time ($T_{INT} < 7$ ms) to achieve high imaging rates and true micro-scanning, high instantaneous dynamic range (+ 50 °C) to accurately image objects much hotter than the background. They also need small pitch FPAs (< 25 μm) in order to get compact and low cost systems.

In this context, parameters such as specific detectivity (D^*) or ultimate background limited (BLIP) performance are no more relevant. Moreover, FPA uniformity, peak wavelength reproducibility, process mastering, play an important role. These are reasons why at TRT research relies on production facilities.

The growth of the active layers is performed in a newly purchased RIBER 49 multi-wafer system. 3 inch wafers as well as 4 inch wafers can be used. Automated wafer charging ensures high yield, suitable for production activities. Arsenic and antimony-based materials can be grown, on different substrates (GaAs, InP, GaSb, InSb, ...). Excellent uniformity on 4 inch wafers is guaranteed and high growth rate stability has been demonstrated [1].

The technological process relies on dry-etching techniques. The quality of the technique can be assessed by controlling the conservation of the current density when varying the pixel size. An example is given in Fig. 1, for nominal pixel sizes ranging from 70 μm down to 10 μm. This study can be completed with low temperature dark current measurements, in order to detect leakage currents. On regular QWIP structures detecting around 9 μm, the leakage currents, if any, are below the detection limit of our experimental setup.

Apart from technological considerations, third generation IR applications also need pertinent physical and optical modelling of the elementary pixel. In the second section of this article we briefly expose our approach on this subject.

Also, it is well known that QWIPs need an optical coupling structure in order to absorb normal incidence

* Corresponding author. Tel.: +33 1 69 41 57 61; fax: +33 1 69 41 57 38.
E-mail address: alexandru.nedelcu@3-5lab.fr (A. Nedelcu).

1350-4495/$ - see front matter © 2006 Elsevier B.V. All rights reserved.
doi:10.1016/j.infrared.2006.10.011

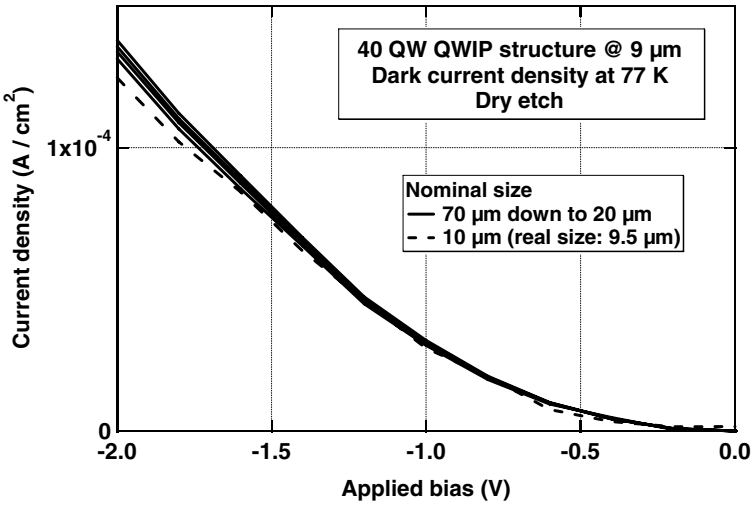

Fig. 1. Dark current density conservation for variable size pixels.

radiation [4,5]. We show in the third section that simple optical coupling structures lead to polarization sensitive detectors. The performance achieved is compatible with realistic applications even for small size pixels.

QWIPs are well suited to take up the challenges of the third generation IR FPAs. Their narrow response is a great advantage for dual-band or dual-color detection. Low spectral cross-talk can be obtained without any constraint on the thickness of the active layers [6,7]. In the fourth section we will present results obtained on building blocks for dual-color detection in the 3–5 µm range.

2. Optical and physical modelling of the elementary pixel: general considerations

Actual system requirements draw technological efforts towards small size pixels, in order to increase spatial resolution and system compactness [3]. It soon appeared that the optical coupling scheme and the size reduction strongly affect the detector responsivity [8]. For 2D gratings a decrease in the coupling efficiency is expected when the number of grating periods is reduced. Fortunately, for small pixels this decrease will be partly compensated by finite size effects, also called edge effects.

The onset of finite size effects depends on the peak wavelength. For 2D gratings the pertinent physical quantity is the number of periods one can etch on each pixel. Short wavelength detectors will then be less affected by the pixel size.

Fig. 2 illustrates the influence of the optical coupling scheme and pixel size on the spectral shape. The sample considered here is a 20 periods $Al_{0.27}Ga_{0.63}As/GaAs$ QWIP structure, detecting at 8.5 µm. Measurements were performed at 77 K and 12 kV/cm, close to the optimum bias set point with respect to FPA performance.

The use of an optical coupling scheme (here 2D gratings) strongly reduces the full-width at half maximum (FWHM). Reducing the pixel size (here from 100 µm down to 20 µm) may shift the peak position and slightly increases FWHM.

Fig. 3 illustrates the influence of the pixel size on the peak responsivity of the same sample. The reduced number of grating periods for small pixels is responsible for the observed responsivity drop. Also, pixels without gratings show an increase in responsivity when size is reduced, due to a higher influence of edge effects [9].

The experimental data gathered lead us to the following conclusions. First, in order to properly asses the FPA performance, electro-optical measurements have to be performed on pixels identical to those forming the FPA (same size, same optical coupling). Use of different optical geometries may lead to wrong quantum efficiency estimation as well as wrong spectral cross-talk values [6]. Second, the optimum active layer and the optimum optical coupling will depend on the pixel size. One cannot dissociate the active layer from the optical coupling when performing optimisation studies.

In most practical cases (e.g. 25 µm pitch) the finite size effects cannot be neglected. The pixel is actually a 3D object whose dimensions compare to the wavelength. As a result, the pixel has to be regarded as a scattering object rather than a periodic structure. Moreover, near field rather than far field is what really matters in determining the optical coupling [9]. In this case usual 2D modelling (e.g. modal expansion method) only provides a qualitative picture. A full and accurate model needs 3D rigorous electro-magnetic capabilities. At TRT we chose a method based on finite difference time domain (FDTD) algorithms and implemented it on a parallel computing platform.

As for the active layer, it is now well established that the quantum wells (QWs) in the structure are not equivalent. First, the incident EM field normal to the QWs is stronger close to the optical coupling structure (near field, [9]). Second, the applied electric field is not constant in the structure due to injection barriers [10]. This will affect the optimum number of quantum wells as well as the optimum

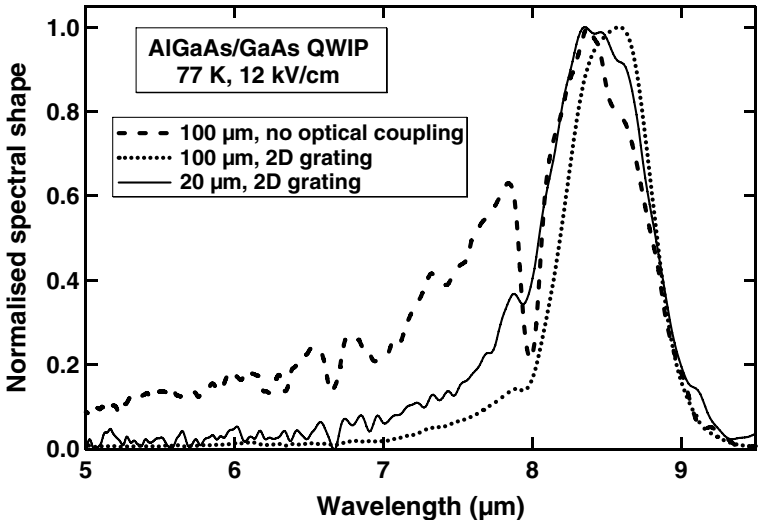

Fig. 2. Influence of the optical coupling and pixel size on the spectral shape.

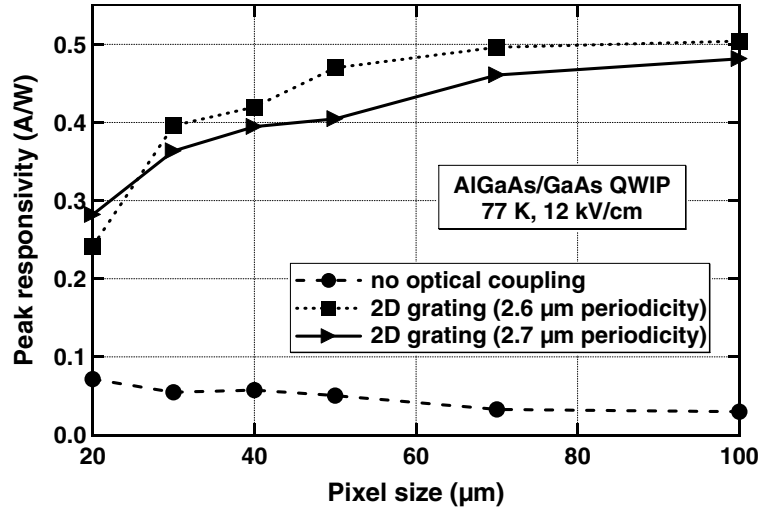

Fig. 3. Influence of the pixel size on the peak responsivity.

doping. Nonuniform structures [11] may lead to improved performance.

3. Building blocks for polarization sensitive FPAs

Exploitation of infrared polarization signatures can enhance the detection probability of man-made objects, whose surface characteristics carry the stamp of their origin. Using appropriate designs of the optical coupling, QWIPs can be easily turned into polarization sensitive detectors [12,13]. The polarizer is thus part of the FPA, leading to simpler and robust imaging systems.

In the following we concentrate on linear gratings for which only the polarization along the modulation direction is effectively absorbed. We studied a 40 periods $Al_{0.27}Ga_{0.63}As/GaAs$ QWIP structure, with response peak around 8.5 μm. Linear gratings with 2.6 μm and 2.7 μm periods were etched on pixels with sizes ranging from 100 μm down to 20 μm. Responsivity measurements were performed using a FTIR and a beam polarizer made from three GaAs plates at the Brewster angle. Polarization insensitive 2D gratings have also been studied, in order to check the experimental setup.

Fig. 4 shows the spectral responsivities for a 20 μm pixel, measured with incident light polarization parallel (TM) or perpendicular (TE) to the gratings (see also inset in the figure). We measure a strong response anisotropy. Yet, the responsivity for parallel polarization is not zero due to finite size effects.

In order to properly asses the detector performance, we introduce the polarization ratio (PR) defined by the following formula:

$$\mathrm{PR} = \frac{I_{\mathrm{TE}} - I_{\mathrm{TM}}}{I_{\mathrm{TE}} + I_{\mathrm{TM}}}$$

We define I_{TE} and I_{TM} as the optical currents corresponding to a fully polarized 300 K background. They can be

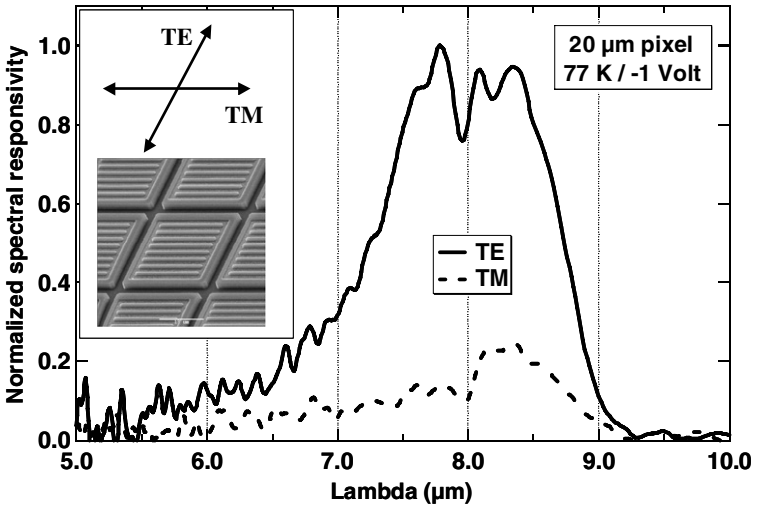

Fig. 4. Spectral responsivity (polarized light) for a 20 μm pixel; TE: beam polarized along the modulation direction; TM: beam polarized along the grating strips. Inset: linear grating geometry.

calculated from the experimental spectral responsivities measured with a polarized beam. As the blackbody emittance is almost constant over the QWIP spectral range, the optical currents are proportional to the integrals of the spectral responsivities.

Fig. 5 shows the evolution of the polarization ratio with the pixel size. As expected, 2D gratings lead to a very low residual polarization ratio (<3%), which is the resolution limit of our experimental setup. For linear gratings the polarization ratio slightly decreases with pixel size. Values larger than 60% are obtained, even for pixels as small as 20 μm. It is worth noting that PR hardly depends on the grating period.

The PR decrease with pixel size can be explained in the following way. When size is reduced, the coupling efficiency of the grating, polarization dependent, is reduced. On the other hand, edge effects, insensitive to polarization, are increased. The overall effect will be a decrease of PR.

The results obtained are very encouraging. The next step will be to build a polarization sensitive FPA. We chose a 20 pitch, 640 × 512 format for the future demonstrator. Different focal plane geometries can be envisaged, two examples are given in the inset of Fig. 5.

4. Building blocks for mid-wave dual-color detection

Dual-band (e.g. 3–5 μm/8–12 μm) and dual-color (e.g. 3–4.2 μm/4.2–5 μm) infrared detection are thought to bring valuable aid to scene interpretation, through reduced dependence on atmospheric conditions and enhanced sensitivity to particular object characteristics such as reflectance, emissivity, absolute temperature. Airborne IR systems could get valuable aid from dual-color detection in the mid-wave IR range (3–5 μm).

The peak wavelength of the QWIP detectors can be easily tailored by properly choosing the well width and the

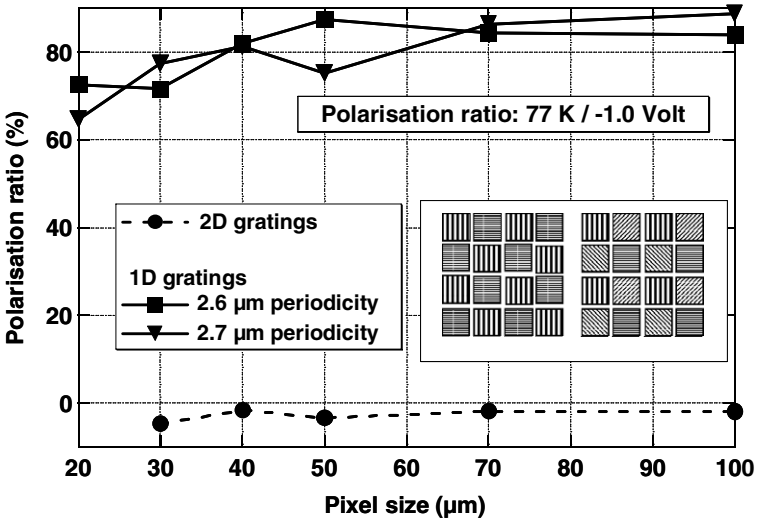

Fig. 5. Evolution of the polarization ratio with pixel size. Inset: two possible FPA geometries.

potential barrier height. To reach wavelengths lower than 4 μm, barrier heights larger than 400 meV (ground state + transition energy) are needed. Conventional AlGaAs/GaAs structures are not well suited for this purpose, due to $\Gamma - X$ crossover for aluminium contents above 40%. On GaAs substrates one generally uses AlGaAs/InGaAs structures.

However, joint use of GaAs substrates and InGaAs alloys leads to strained epilayers. One has to limit the global indium content and layer thickness in order to avoid elastic relaxation and dislocations. To bypass this problem, we designed AlGaAs/AlAs/InGaAs/AlAs/AlGaAs structures [14]. We use AlAs layers in order to increase the confinement energy of the excited states. This allows us to limit the indium content to less than 25%. A low indium content, together with the use of a small number of wells (5–10), allows us to keep the applied biases compatible with existing read-out circuitry. Well width, and exact barrier and well alloy compositions are chosen according to the desired peak wavelength. Based on this structure, different layers have been designed, covering the whole 4–5 μm spectral range (see Fig. 6).

In the following we will present our first results on the electro-optical characteristics measured on a 4 μm structure. It contains 5 QWs, and the nominal doping is 1×10^{12} cm^{-2}. A sketch of the conduction band structure at Γ point is given in Fig. 7.

Fig. 8 shows the current-voltage characteristics measured on a 23 μm pixel. Dark current is thermally activated in the range 80 K–110 K. The activation energy is 260 meV at zero bias, in fair agreement with the value deduced from the responsivity peak position (310 meV) and the estimated Fermi energy (40 meV). This suggest that the excited state lies close to the top of the well (bound to quasi-bound transition). For a f/2 aperture and a 293 K background the BLIP temperature is 95 K at −1.2 V.

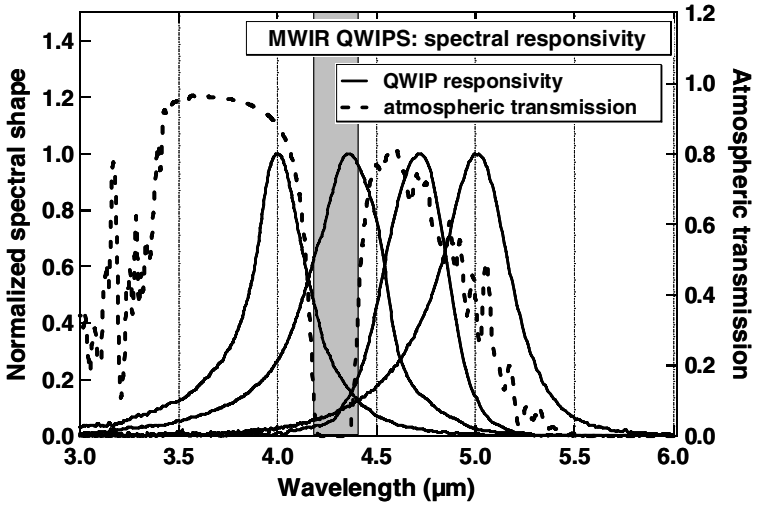

Fig. 6. Spectral responsivities for MWIR QWIPS. Dotted line: transmission of a 5000 m thick atmospheric layer; grey area: CO_2 absorption band.

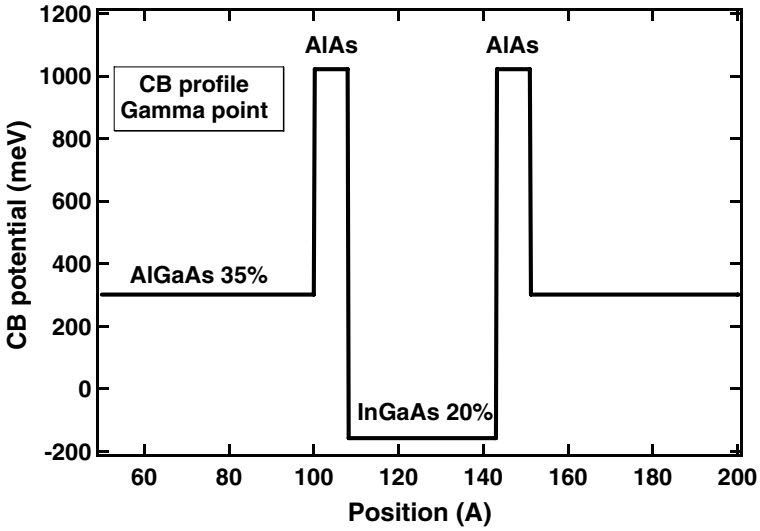

Fig. 7. Γ-point potential profile for a MWIR QWIP with peak response at 4 μm.

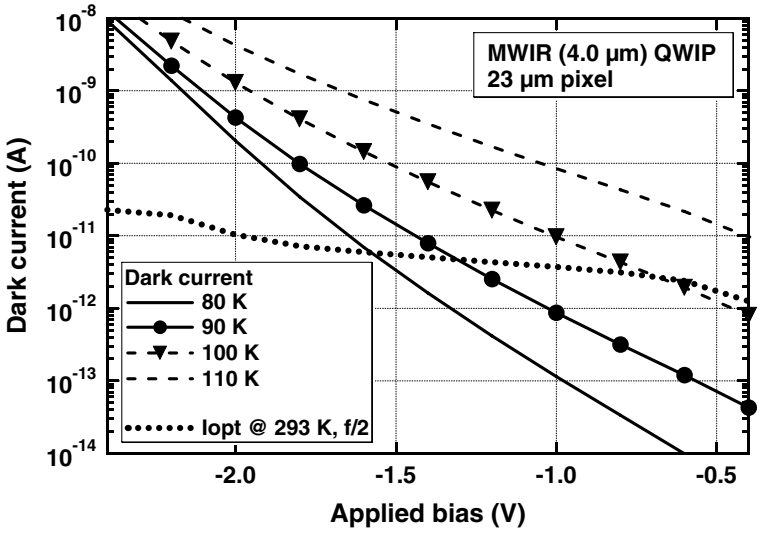

Fig. 8. Current–voltage characteristics for a 23 μm QWIP pixel, with peak response at 4 μm.

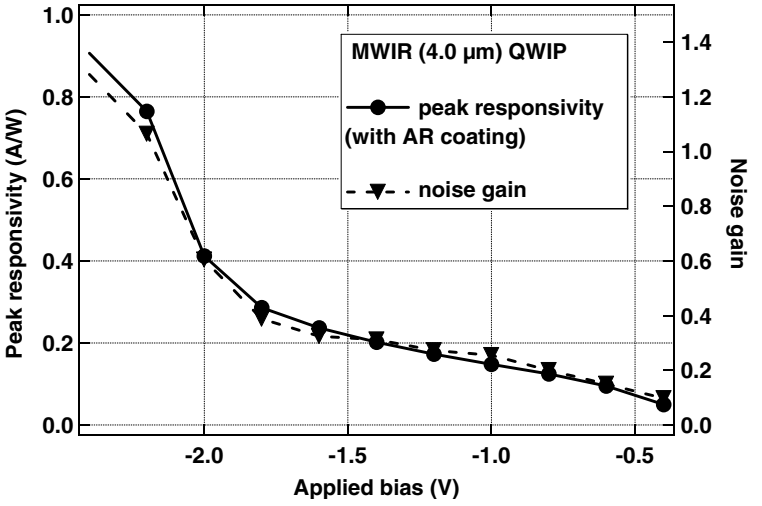

Fig. 9. Peak responsivity and noise gain for a 23 μm QWIP pixel, with peak response at 4 μm.

Fig. 9 shows the peak responsivity and noise gain (extracted from noise measurements assuming a simple photoconductive model). In the presence of an anti-reflection coating, the peak quantum efficiency reaches 20% and is bias independent. We also notice that the noise gain sharply increases above 2 Volts. This may be the signature of extra noise sources, such as impact ionisation [15,16], which add to classical generation-recombination noise [17].

The sample studied is our first QWIP structure below 4 μm and we think there is room for performance improvement. Future studies will aim at increasing the quantum efficiency, by modifying the number of wells, as well as the well doping. We will also attempt to further lower the peak wavelength.

5. Conclusion

After intensive work to raise the FPA temperature in order to bring QWIP technology into systems, we now concentrate on other interesting capabilities. We have presented here the present research topics on third generation quantum well IR detectors at Thales Research and Technology. We stress the importance of pertinent modelling for detector optimisation and also the importance of pertinent electro-optical characterization for performance assessment. We present experimental results on small size (20 μm), polarization sensitive pixels and demonstrate the maturity of the present building blocks.

Finally, we present our first results on short wavelength (4 μm) QWIPs, intended for dual-color MWIR/MWIR detectors.

References

[1] E. Costard, A. Nedelcu, X. Marcadet, E. Belhaire, P. Bois, Proc. SPIE Int. Soc. Opt. Eng. (2006) 6206–6213.
[2] A. Manissadjian, D. Gohier, E. Costard, A. Nedelcu, Proc. SPIE Int. Soc. Opt. Eng. (2006) 6206–6214.

[3] S. Crawford, R. Craig, A. Haining, J. Parsons, E. Costard, P. Bois, F.H. Gautier, O. Cocle, Proc. SPIE Int. Soc. Opt. Eng. (2006) 6206–6217.
[4] K.W. Goossen, S.A. Lyon, K. Alavi, Appl. Phys. Lett. 53 (1988) 1027.
[5] J.Y. Andersson, L. Lundqvist, Appl. Phys. Lett. 59 (1991) 857.
[6] A. Nedelcu, X. Marcadet, O. Huet, P. Bois, Appl. Phys. Lett. 88 (2006) 191113.
[7] P. Castelein, F. Guellec, F. Rothan, S. Martin, P. Bois, E. Costard, O. Huet, X. Marcadet, A. Nedelcu, Proc. SPIE Int. Soc. Opt. Eng. 5783 (2005) 804.
[8] L. Lundqvist, J.Y. Andersson, Z.F. Paska, J. Borglind, D. Haga, Appl. Phys. Lett. 63 (1993) 3361.
[9] A. De Rossi, E. Costard, N. Guerineau, S. Rommeluere, Infrared Phys. Technol. 44 (2003) 325.
[10] L. Thibaudeau, P. Bois, J.Y. Duboz, J. Appl. Phys. 79 (1996) 446.
[11] S.Y. Wang, Y.C. Chin, C.P. Lee, Infrared Phys. Technol. 42 (2001) 177.
[12] C.J. Chen, K.K. Choi, L. Rokhinson, W.H. Chang, D.C. Tsui, Appl. Phys. Lett. 74 (1999) 862.
[13] D.W. Beekman, J. Van Anda, Infrared Phys. Technol. 42 (2001) 323.
[14] A. Fiore, E. Rosencher, P. Bois, J. Nagle, N. Laurent, Appl. Phys. Lett. 64 (1994) 478.
[15] H. Schneider, Appl. Phys. Lett. 82 (2003) 4376.
[16] L. Gendron, V. Berger, B. Vinter, E. Costard, M. Carras, A. Nedelcu, P. Bois, Semicond. Sci. Technol. 19 (2004) 219.
[17] W.A. Beck, Appl. Phys. Lett. 63 (1993) 3589.